Progress In Electromagnetics Research M, Vol. 114, 127–137, 2022

A Multifunctional Patch Antenna Loaded with Near Zero Index Refraction Metamaterial

Fatima Zohra Khoutar*, Oumaima Nayat-Ali, Mariem Aznabet, and Otman El Mrabet

Abstract—In this paper a multifunctional patch antenna loaded with near zero index refraction metamaterial (NZIM) is presented. This multifunctional antenna operates at 5.8 GHz and provides high gain and beam steering capability. The proposed configuration comprises a patch antenna placed below an NZIM superstrate. The rectangular microstrip antenna is used as a radiation source to demonstrate the performance of this design. The NZIM superstrate, which behaves as an NZIM, based on 9×9 resonating unit cells of split ring resonators (SRRs), allows gathering radiated waves from the antenna and collimating them toward the superstrate's normal direction, which results in gain enhancement. The beam-steering in the E-plane is obtained by slowly tilting the NZIM over the patch antenna. The main characteristics of the antenna placed near the NZIM superstrate are studied numerically and experimentally to successfully demonstrate this dual function feature. It is found experimentally that the gain enhancement of 8 dB with improved directivity and radiation efficiency are obtained in comparison with the antenna without the NZIM metasurface. In addition, we were also able to steer the direction of the main beam just by tilting the NZIM superstrate from $-20°$ to $20°$ with a gain variation of 5 dB and without changing the whole dimension of the structure.

1. INTRODUCTION

Recently, metamaterial (MTM) structures are the topic of studies by many researchers and have attracted enormous research interest thanks to its potential to control and manipulate the properties of electromagnetic waves. In antenna applications, metamaterials can be used to enhance antenna gain, improve bandwidth and efficiency, reduce backward radiation, and convert polarization. For radiation pattern enhancement, different techniques have been published within the literature in recent years. The conventional way to get a considerable enhancement in the gain is the use of an array of several radiating elements with a specific feeding network [1, 2]. However, this technique makes the total size of the antenna large and suffers from complicated feeding mechanisms which render the whole system more complex with undesired coupling and radiation losses. Another approach is to employ a superstrate of either high permittivity or permeability above the patch antenna [3] which is costly. Artificial materials like frequency selective surfaces (FSSs) and electromagnetic band gap (EBG) structures were also proposed by several researchers for antenna gain improvement [4, 5]. Nevertheless, these techniques increase the overall thickness of the antenna. Partial reflective surfaces (PRSs) linked with an artificial magnetic conductor (AMC) were proposed to overcome this drawback [6, 7]. Thus, the total thickness is decreased using this approach, but the aperture efficiency remains lower.

For beam steering, radiation pattern reconfigurable antennas are used in different applications within electronic engineering like telecommunication and radar. They reduce interference by conducting the antenna's radiation to the direction desired. Conventionally electrical control of beamsteering is

Received 22 September 2022, Accepted 12 November 2022, Scheduled 23 November 2022

* Corresponding author: Fatima Zohra Khoutar (fatikhoutar@gmail.com).
The authors are with the Information and Telecommunication Systems (LaSiT) Laboratory, Faculty of Science, Abdelmalek Essaadi University, Tetuan 93000, Morocco.

realized. However, a fancy feeding network with an outsized number of phase shifters and a biasing network are needed [8]. Additionally, at high frequencies and for high-gain applications systems it suffers from heavy power losses within the feed network and RF components like PIN diodes and phase shifters [9, 10].

Radiation beams in several directions were obtained based on passive metasurfaces with different phase profiles [11, 12]. These configurations supply the main beam in the desired direction, and the beam orientation was fixed for one antenna structure which limits the utility of beam steering. For the purpose of altering the direction of the main beam with the passive metasurface, a simple element is used to excite the metasurface [13, 14]. These structures were initially steering the main beam in a specific direction by changing the position of the metasurface above the planar antenna which enhanced the total size of the structure.

In this paper, we propose a multifunctional patch antenna with a high gain antenna based on near zero index metamaterial structures and with the capability of the beam-steering in the elevation plane without using any active components and without changing the whole dimension of the proposed structure. The proposed beam steering technique is based on the passive Fabry-Perot (FP) cavity antenna [15] configuration by simply tilting the metasurface above the patch antenna.

2. NEAR ZERO INDEX METAMATERIAL DESIGN AND ANALYSIS

The configuration of the SRR unit cell acting as the basic element of the artificial near zero-index metamaterial superstrate is shown in Figure 1. The MTM unit cell (Figure 1(a)) is a split ring resonator formed by a pair of concentric rings with splits at opposite ends printed on both sides of a Rogers RT/Duroid 5880 substrate with thickness of $h_1 = 0.8$ mm, loss Tangent of 0.0004, and relative permittivity of 2.2. The SRR unit cell has an outer square side length of $f = 8$ mm while the width of the etched copper segments is $w = 0.4$ mm. The gap spacing between inner and outer square rings is $d = 0.4$ mm which is equal to the gaps in the square rings ($c = 0.4$ mm). To simulate a periodic array of SRRs placed in the xy plane (Figure 1(b)), a single SRR unit cell is simulated, using CST Microwave studio, with PEC and PMC boundary conditions which are defined in such a way that the electric field is kept along x axis while the magnetic field is kept along y axis. Consequently, the propagation direction of the wave vector k propagates in the z direction.

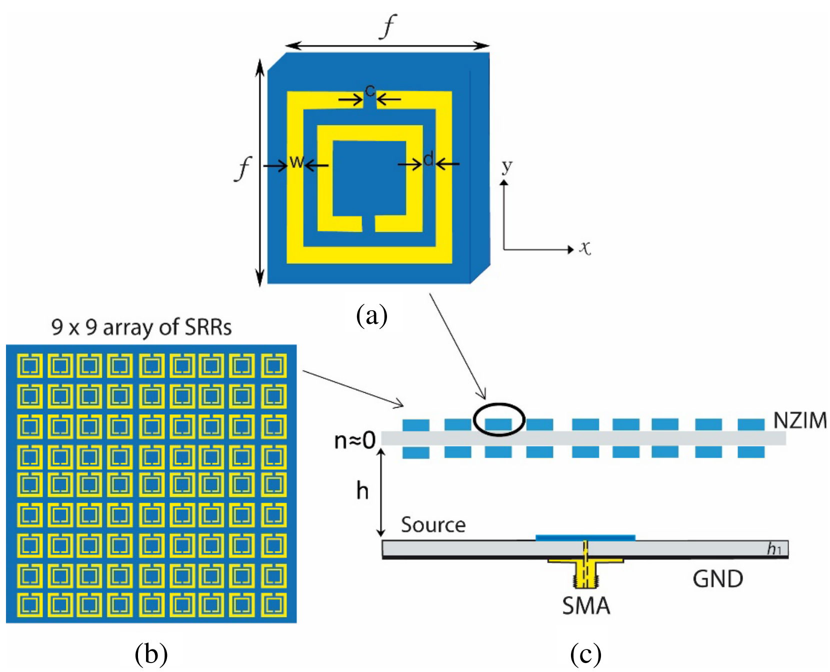

Figure 1. Proposed design. (a) Unit cell, (b) NZIM metasurface, and (c) rectangular patch antenna covered by a NZIM superstrate.

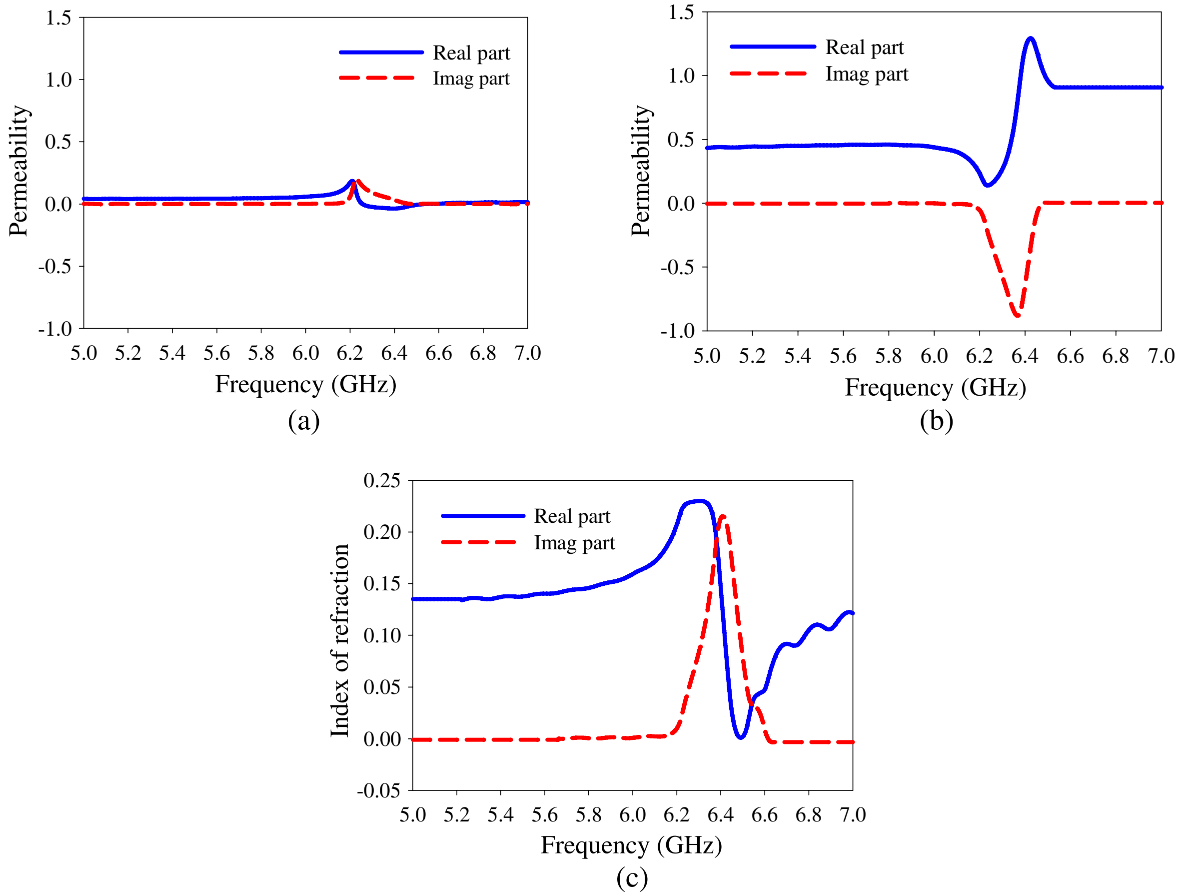

Figure 2. Extracted effective parameters of the unit cell: (a) Permeability, (b) permittivity and (c) refractive index.

From the simulated reflection and transmission coefficients (S_{11} & S_{21}), we can easily get the effective parameter of this structure using the method reported in [16]. The obtained effective parameters of the SRR unit cell are shown in Figure 2 which demonstrate an interesting property of the metamaterial wherein the permeability and permittivity are simultaneously near zero around the resonant frequency of 5.8 GHz. This in turn means that the metamaterial unit cell will have near zero refractive index (NZRI) and constitutes a near zero index-metamaterial (NZIM) unit cell around 5.8 GHz.

This is considering the fact that a slab with a very low (close to zero) index (See Figure 3) has the ability to focus the beam towards the broadside direction. Indeed, according to Snell's law the radiated beam will pass through NZIM medium and experience beam confinement which, in turn, results in enhanced gain. According to Snell's law for an electromagnetic wave propagating from NZIM superstrate to the air medium, the following equation is hold:

$$n_1 \sin\theta_1 = n_0 \sin\theta_0 \tag{1}$$

where θ_1 and θ_0 are the incidence and refraction angle, whereas n_1 and n_0 are the refractive index of NZIM superstrate and air medium, respectively (Figure 3(a)). In the case of NZIM, $n_1 = 0$ but $n_0 \neq 0$ for air medium, then $\theta_0 = 0$, which means that for an incident wave from an NZIM medium into the free space, the angle of refraction will remain close to zero, that is, the refracted wave will be normal to the interface. Thus, using the NZIM superstrate, the phase variation of the electromagnetic waves is extremely small or zero, which results in enhancement of gain. The gain enhancement mechanism of NZIM superstrate is shown in Figure 3(b). Hence, the proposed NZIM can find potential applications in realizing antennas with high gain and directivity.

To determine the height h of the superstrate, that is the distance between the patch antenna and the metamaterial slab, two optimization stages can be done. The first one consists of finding the range of

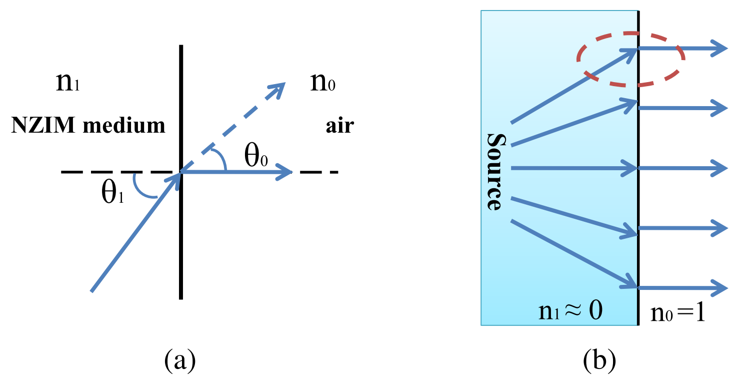

Figure 3. (a) Wave propagation through a normal material and near to zero metamaterials. (b) The gain enhancement mechanism of NZIM.

h where the same resonance frequency of the patch antenna is preserved. The second optimization stage is finding the specific value of h where the maximum realized gain is obtained. Also, the distance h is tuned in order to ensure that the coupling between the patch antenna and superstrate is not significant.

3. NZIM STRUCTURE AS A SUPERSTRATE FOR PLANAR ANTENNA GAIN ENHANCEMENT

Figure 1(c) shows the schematic diagram of the proposed NZIM based high gain antenna which is composed of an NZIM superstrate and a rectangular planar patch antenna considered as a primary source. The rectangular planar antenna is fed through a $50\,\Omega$ coaxial probe and printed on a grounded substrate of Rogers RT/Duroid 5880, measuring $72 \times 72\,\text{mm}^2$, with permittivity of 2.2, loss tangent of 0.004 and thickness of $h_1 = 0.8\,\text{mm}$. The rectangular planar antenna was optimized with a series of the CST Microwave simulations to get a low profile and an operating band around the center frequency of 5.8 GHz. The NZIM metasurface with dimensions $72 \times 72 \times 1.6\,\text{mm}^3$ accommodates a 9×9 periodic array of SRRs as shown in Figure 1(b). It is placed at the height of $h = 30\,\text{mm}$ from the rectangular planar patch antenna. As discussed in the previous section, this NZIM metasurface exhibits a near zero index metamaterial around the resonant frequency of 5.8 GHz, and according to Snell's law, radiation from a fixed rectangular patch antenna incident on the NZIM metasurface with any angle will be refracted with a very small angle towards the broadside direction. This focusing scheme of NZIM metasurface can increase the gain of the rectangular patch antenna by 8-dB.

Parametric study has been performed to study the effects of the separation distance h between the antenna and the metasurface on the resonant frequency and broadside gain. The obtained results are presented in Figure 4. It is found that the resonant frequency can be changed, when the height h (distance between NZIM and ground plane) is decreased from about 0.5λ down to 0.4λ, 0.3λ and 0.1λ. This result shows that the parameter h plays an important role in tuning the resonant frequency of the structure.

It is also seen from Figure 4(b) that when h equals 0.3λ and 0.1λ, respectively, the antenna gain is degraded. However, with increasing the superstrate height to about 0.5λ, the broadside gain is enhanced. Thus, the maximum gain with better bandwidth and good impedance matching is obtained for an optimized value of the h about 0.5λ. The overall thickness of 30 mm has been achieved for the proposed antenna configuration which is $\lambda/2$. Furthermore, numerical simulations are performed to study the effect of the area of the metasurface (the number of unit cells in metasurface) on the broadside gain. The Comparison of the broadside gains of the antenna loaded with different NZIM metasurface areas is listed in Table 1. It is clearly observed that the broadside gain of the proposed antenna gradually increases with the increase in the number of unit cells. However, a finite array of 9×9-unit cell is chosen as an optimized combination of the MTM superstrate. The maximum gain of

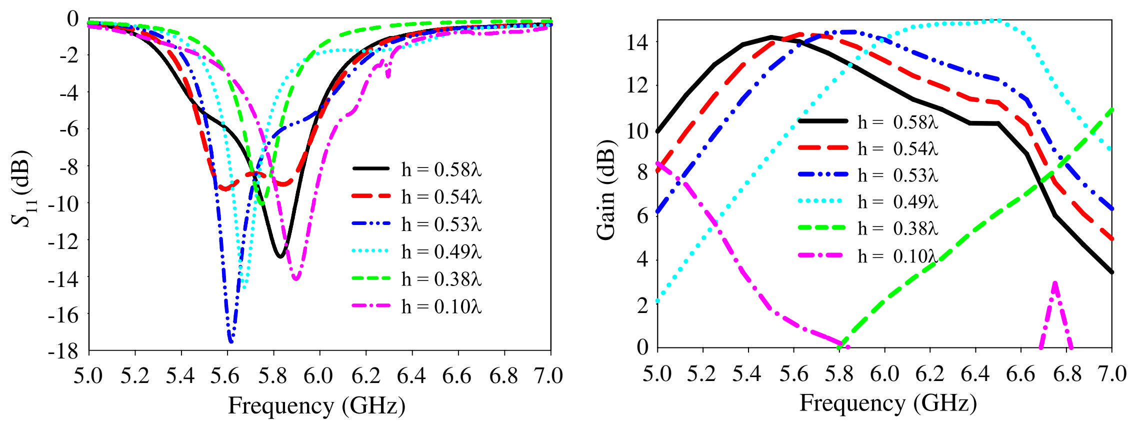

Figure 4. Effect of the separation distance h: (a) Simulated reflection coefficient and (b) gain of the antenna with NZIM metasurface for various separation distance h.

Table 1. Gain variation with the number of SRR unit cell.

	Gain	**Frequency**
7×7-unit cells	11.23	5.8
8×8-unit cells	12.08	5.8
9×9-unit cells	13.72	5.8

the antenna can be approximated by the formula of the ideal radiating openings given in [17]:

$$G = 10 \log \left(\frac{4\pi}{\lambda^2} S \right) \tag{2}$$

where $\lambda = 51.72\,\text{mm}$ and $S = 5184\,\text{mm}^2$ are the operating wavelength of the microstrip patch antenna (MPA) and the square surface formed by the structure, respectively. Based on Equation (2) we obtain a gain of $G = 13.86\,\text{dB}$. So, the length and width of the MTM layer are taken in such a way that it can effectively cover the broadside radiation of patch. Finally, we can say that the height h and the area of the NZIM metasurface are key parameters on antenna gain enhancement.

4. STEERING ANTENNA BEAM IN CAVITY FABRY PEROT

A new method of beam steering is presented here (Figures 5(a) and (b)), and the idea is steering the main beam of the antenna by titling the NZIM superstrate around the Z-axis.

Compared with the literature [18, 19], the advantage of this method is keeping the overall volume $(1.2\lambda\times1.2\lambda\times0.5\lambda)$ of the proposed structure unchanged throughout the beam-steering operation without using any active components.

The radiation patterns, showing the beam-steering in the E-plane by slowly rotating the NZIM around the Z-axis, are depicted in Figure 6. It is found that for a small range of titling angle, starting from $\theta_0 = 0°$ to $\theta_0 = 20°$ with 2 steps, the NZIM steers the direction of main beam from $\theta = 0°$ to $\theta = -20°$ in the E-plane. Note that if the MTM superstrate is tilted in the inverse directions, the beam steering angle range of $0°$ to $20°$ degrees can be realized.

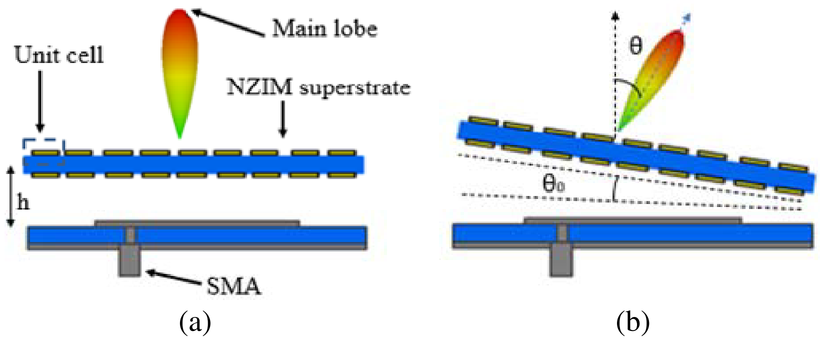

Figure 5. Schematic configurations of the proposed structure: (a) The beam in the broadside direction, (b) the beam in the off-normal direction.

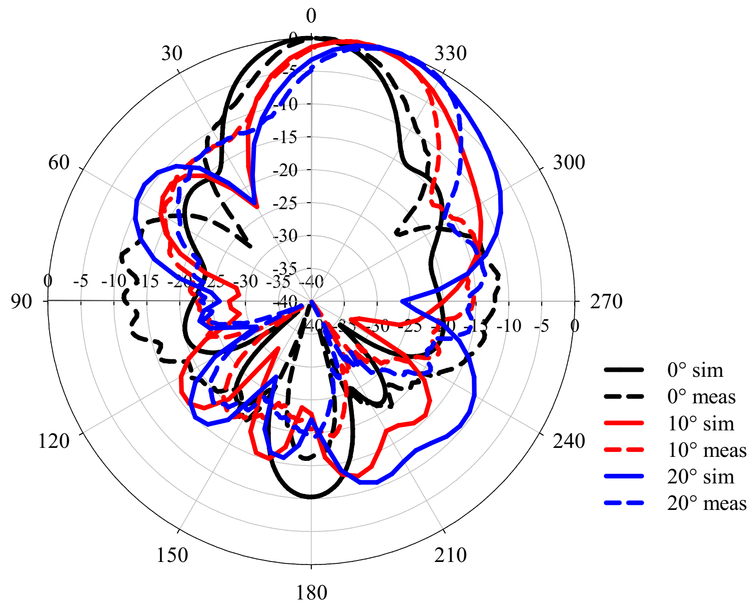

Figure 6. Simulated and measured far field normalized radiation pattern of the proposed antenna with NZIM metasurface for different value of θ_0.

5. MEASUREMENT AND DISCUSSION

To verify the design concept, a prototype of the high gain antenna was fabricated using an LPKF Protomat S100 mill/drill unit, and its characteristics are experimentally analyzed to verify the obtained simulation results. The top view of the fabricated reference antenna (rectangular microstrip patch antenna) is shown in Figure 7(a). The fabricated prototype of the NZIM metasurface is depicted in Figure 7(c), and the antenna with the NZIM metasurface is shown in Figure 7(b). The single layer NZIM superstrate is placed above the reference patch antenna at a height of $h = 30$ mm.

Note that the separation between the antenna and NZIM metasurface is maintained by using four acrylic screws (included in the simulations). The measured and simulated reflection coefficients of the rectangular patch antenna with and without NZIM metasurface are plotted in Figure 8 for the ease of comparison. Small discrepancy can be observed between the two sets of data. This can be ascribed to tolerances in the dielectric permittivity, connector losses, and tolerances in the fabrication process. The measured results show that the bandwidth of the rectangular patch antenna without the metasurface ranges from 5.74 to 5.81 GHz; however, the one with metasurface exhibits a bandwidth ranging from

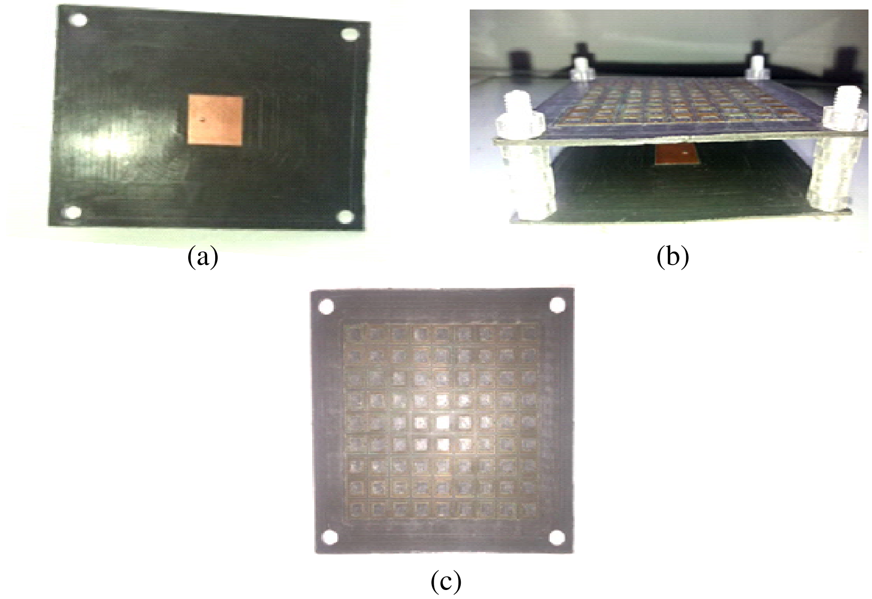

Figure 7. Fabricated prototype of the proposed high gain antenna: (a) Rectangular patch antenna, (b) proposed high gain antenna, and (c) double sided 9 by 9 NZIM unit cells.

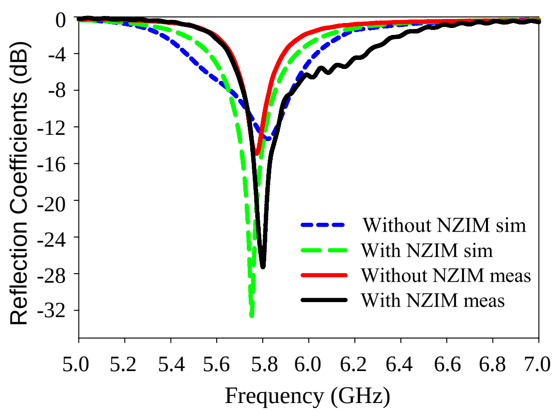

Figure 8. Simulated and measured reflection coefficient of the proposed antenna with and without NZIM metasurface.

5.74 to 5.93 GHz. This means that 1.5% improvement in the impedance matching bandwidth is achieved by the use of presented NZIM.

To demonstrate the performance of the high gain antenna in free space, its far field normalized radiation patterns of E- and H-planes have been measured at the resonance frequency of 5.8 GHz. The obtained results are plotted in Figure 9. The simulated and measured radiation patterns are seen to agree well with each other and show that the directivity of the antenna with NZIM metasurface has been increased significantly for both E- and H-planes.

Examining Figure 9, we can observe that the main lobe is as expected in the direction of the positive z-axis (the direction of propagation) and that the back-lobe level decreases, and broadside level increases in the case of the antenna loaded with NZIM metasurface. Hence, loading a microstrip antenna with NZIM metasurface has an important effect on the reduction of the -3 dB beam width. It is found that the beamwidth decreases from $104°$ to $28.3°$ in the E-plane and from $83.5°$ to $30.4°$ in the H-plane. The reduction in 3-dB beamwidth indicates an enhancement in directivity in the broadside direction and the sharpening of radiation pattern main lobe.

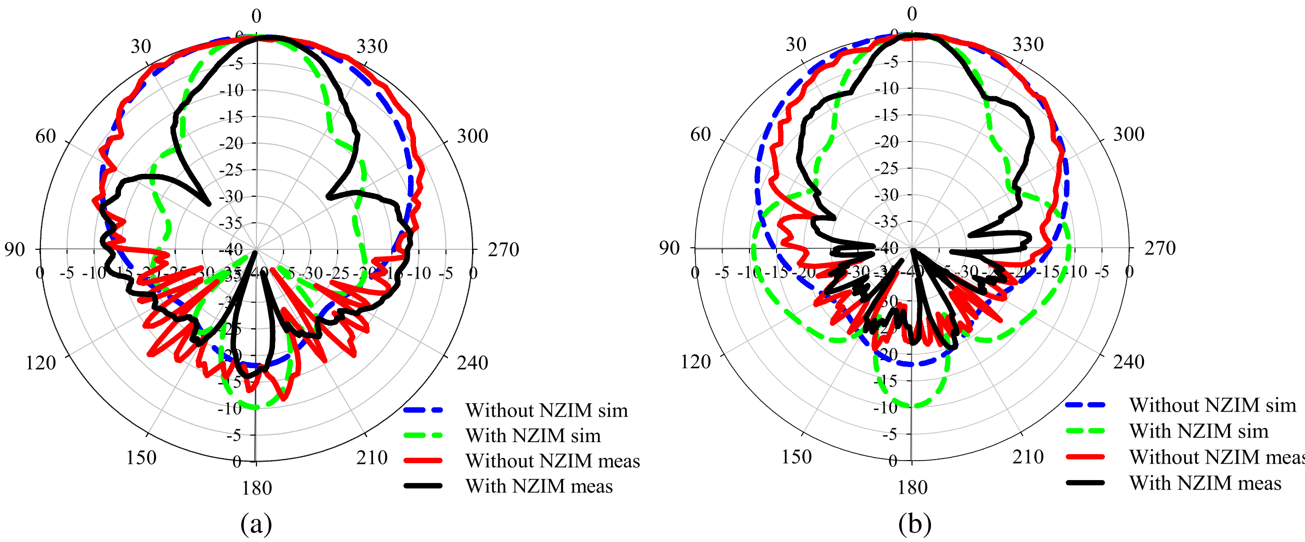

Figure 9. Simulated and measured far field normalized radiation pattern of the antenna with and without NZIM metasurface. (a) *E*-plane. (b) *H*-plane.

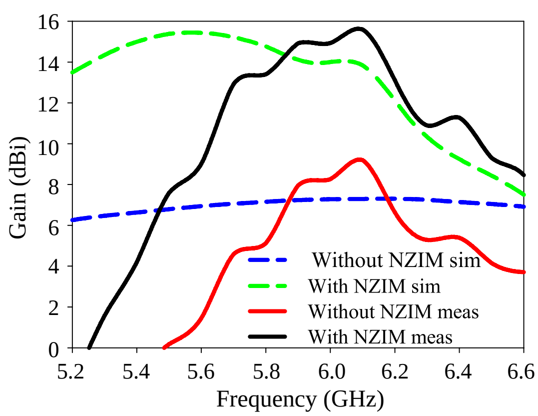

Figure 10. Measured and simulated gain of the antenna with and without NZIM metasurface as a function of frequency.

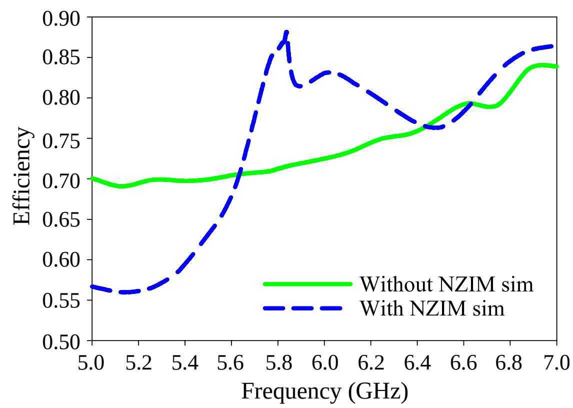

Figure 11. Simulated radiation efficiency of the antenna with and without NZIM metasurface as a function of frequency.

To further corroborate this effect, measured and simulated gains of the antenna with and without NZIM metasurface as a function of frequency are also conducted, and the obtained results are compared in Figure 10. Some slight discrepancies between the measured and simulated results have been observed. These may be ascribed to fabrication errors and alignment difficulties of the high gain antenna and feed. Also, an improvement in gain due to the incorporation of the NZIM metasurface is noted. Comparing the measured and simulated gains of the antenna with and without the NZIM metasurface, about 8.3 dB increase of the gain measured is observed around the resonant frequency of 5.8 GHz. The increase in gain can be explained by parametric analysis data presented in the above section, where the major contributing factor to the increase of gain is the increase in the effective aperture area of the antenna and due to placement of the superstrate which is an MTM superstrate acting as an NZIM superstrate.

The simulated radiation efficiencies of the rectangular patch antenna with and without the NZIM metasurface are presented in Figure 11. At the resonance frequency of 5.8 GHz, the antenna without NZIM metasurface attained and expected low radiation efficiency of 71%, and the one with NZIM metasurface shows a high radiation efficiency of 85%.

To assess the novelty of the proposed design, it is compared with other earlier structures published

Table 2. Comparison of the proposed design with other structures for gain enhancement.

Ref.	Freq. (GHz)	Distance of superstrate from patch (mm)	Gain Enhancement (dB)	Aperture efficiency	Type and number of Superstrate
[20]	10–12.4	$0.5\lambda_0$	4.5	65.20%	Transmission, 2
[21]	10.8	$0.5\lambda_0$	6.95	83.00%	Transmission, 1
[22]	4.5	$0.5\lambda_0$	5.5	–	Transmission, 1
[23]	9.35	$2.8\lambda_0$	2.7	–	Transmission, 6
[24]	5.9	$0.5\lambda_0$	7.6	–	Transmission, 4
[25]	4	$0.5\lambda_0$	1.94	95%	Transmission, 1
[26]	6.8–9.6–15.4	$0.4\ \lambda_0$	4.4	–	Transmission, 3
This work	5.8	$0.5\lambda_0$	8.3 dB	85.00%	Transmission, 1

in the literature for gain enhancement by employing metamaterial structures. The comparative study is summarized in Table 2. It is observed from the table that the gain enhancement of our proposed design is much better than other works also for very high radiation efficiency, and it can be useful for high directivity application. For [26] the antenna is wideband compared with our work, but the gain enhancement is smaller. In addition, our proposed structure provides a gain enhancement with a beam steering capability. Furthermore, unlike all reported designs (see Table 2), for to the best of the authors' knowledge, up to now there is no previously published work that reports the same achievements presented in our work. Thus, the proposed work is novel in terms of designing a compact and higher gain metamaterial antenna resulting into high aperture efficiency compared to other similar reported works with a capability of beam steering.

6. CONCLUSIONS

In this paper, a multifunctional patch antenna loaded with near zero index refraction metamaterial (NZIM) is designed, fabricated, and measured for wireless communication systems. The experimental results reveal that the introduction of the NZIM metasurface placed at the optimum height of 0.5λ from the reference source increases the gain by 8-dB at the resonant frequency with aperture efficiency of 85%. It is also found that the radiation efficiency has been increased by introducing the NZIM superstrate. More interestingly, the beam-steering in the E-plane has been obtained by slowly tilting the NZIM superstrate above the patch antenna. It is worth to mention that for practical applications the beam steering can be done mechanically. The proposed structure may find applications in different wireless communication systems that need beam steering along with high gain performances.

REFERENCES

1. Ghassemi, N. and K. Wu, "High-efficient patch antenna array for E-band gigabyte point-to-point wireless services," *IEEE Antennas Wirel. Propag. Lett.*, Vol. 11, 1261–1264, Oct. 2012.
2. Kim, D. Y., Y. Lim, H. S. Yoon, and S. Nam, "High-efficiency W-band electroforming slot array antenna," *IEEE Trans. Antennas Propag.*, Vol. 63, 1854–1857, Apr. 2015.
3. Nasimuddin, K. Esselle, and A. K. Verma, "Compact circularly polarized enhanced gain microstrip antenna on high permittivity substrate," *Asia-Pacific Microwave Conference Proceedings*, Mar. 2006.

4. Munk, A. B., *Frequency Selective Surfaces: Theory and Design*, John Wiley & Sons, Hoboken, Jan. 2005.
5. Lee, Y. J., J. Yeo, R. Mittra, and W. S. Park, "Design of a high-directivity electromagnetic band gap (EBG) resonator antenna using a frequency-selective surface (FSS) superstrate," *Microw. Opt. Technol. Lett.*, Vol. 43, 462–467, Oct. 2004.
6. Yang, F. R., K. P. Ma, Y. Qian, and T. Itoh, "A uniplanar compact photonic-bandgap (UC-PBG) structure and its applications for microwave circuit," *IEEE Trans. Microw. Theory Techn.*, Vol. 47, 1509–1514, Aug. 1999.
7. Yuehe, G., P. E. Karu, and S. B. Trevor, "The use of simple thin partially reflective surfaces with positive reflection phase gradients to design wideband, low-profile EBG resonator antennas," *IEEE Trans. Antennas Propag.*, Vol. 60, 743–750, Oct. 2012.
8. Nikfalazar, M., et al., "Two-dimensional beam-steering phased-array antenna with compact tunable phase shifter based on BST thick films," *IEEE Antennas Wirel. Propag. Lett.*, Vol. 16, 586–588, 2017.
9. Aslan, Y., J. Puskely, J. H. J. Janssen, M. Geurts, A. Roederer, and A. Yarovoy, "Thermal-aware synthesis of 5G base station antenna arrays: An overview and a sparsity-based approach," *IEEE Access*, Vol. 6, 58868–58882, 2018.
10. Abdellatif, A. S. M., "High performance integrated beam-steering techniques for millimeter-wave systems," *Univ. Waterloo*, Waterloo, ON, USA, 2015.
11. Ghasemi, A., et al., "High beam steering in Fabry-Perot leaky-wave antennas," *IEEE Antennas Wirel. Propag. Lett.*, Vol. 12, 261–264, 2013.
12. Nakano, H., S. Mitsui, and J. Yamauchi, "Tilted-beam high gain antenna system composed of a patch antenna and periodically arrayed loops," *IEEE Trans. Antennas Propag.*, Vol. 62, 2917–2925, 2014.
13. Katare, K. K., A. Biswas, and M. J. Akhtar, "Microwave beam steering of planar antennas by hybrid phase gradient metasurface structure under spherical wave illumination," *J. Appl. Phys.*, Vol. 122, 234901, 2017.
14. Katare, K. K., A. Biswas, and M. J. Akhtar, "Wideband beam-steerable configuration of metasurface loaded slot antenna," *Int. J. RF. Microwave Comput. Aid Eng.*, e21408, 2018.
15. Trentini, G. V., "Partially reflecting sheet array," *IRE Trans. Antennas Propag.*, Vol. 4, 666–671, 1956.
16. Chen, X., M. T. Grzegorczyk, B. I. Wu, J. Pacheco, Jr., and J. A. Kong, "Robust method to retrieve the constitutive effective parameters of metamaterials," *Phys. Rev. E*, Vol. 70, 16608, Jul. 2004.
17. Li, D., Z. Szabó, X. Qing, E. Li, and Z. N. Chen, "A high gain antenna with an optimized metamaterial inspired superstrate," *IEEE Trans. Antennas Propag.*, Vol. 60, 6018–6023, Aug. 2012.
18. Reis, J. R., M. Vala, T. E. Oliveira, T. R. Fernandes, and R. F. S. Caldeirinha, "Metamaterial-inspired flat beamsteering antenna for 5G base stations at 3.6 GHz," *Sensors*, Vol. 21, 8116, Dec. 2021.
19. Luo, Y., Q. Zeng, X. Yan, T. Jiang, R. Yang, J. Wang, Y. Wu, Q. Lu, and X. Zhang, "A graphene-based tunable negative refractive index metamaterial and its application in dynamic beam-tilting terahertz antenna," *Microw. Opt. Technol. Lett.*, Vol. 61, No. 12, 2766–2772, Dec. 2019.
20. Kumar, S., L. Kurra, M. Abegaonkar, A. Basu, and S. K. Koul, "Multilayer FSS for gain improvement of a wide-band stacked printed antenna," *2015 International Symposium Antennas Propagation (ISAP)*, 1–4, Hobart, TAS, 2015.
21. Kurra, L., M. P. Abegaonkar, A. Basu, and S. K. Koul, "FSS properties of a uniplanar EBG and its application in directivity enhancement of a microstrip antenna," *IEEE Antennas Wirel. Propag. Lett.*, Vol. 15, 1606–1609, 2016.
22. Zhu, H., S. W. Cheung, and T. I. Yuk, "Enhancing antenna boresight gain using a small metasurface lens: Reduction in half-power beamwidth," *IEEE Antennas Propag. Mag.*, Vol. 58, 35–44, Feb. 2016.

23. Ma, B., X. M. Yang, T. Q. Li, H. Y. Chenc, H. Hed, Y. W. Chend, A. Line, J. Chenf, and B. J. Wangg, "Gain and directivity enhancement of microstrip antenna loaded with multiple splits octagon-shaped metamaterial superstrate," *Int. J. Appl. Electromagn.*, Vol. 58, 201–213, 2016.
24. Gangwar, D., D. Sushrut, and R. L. Yadava, *Gain Enhancement of Microstrip Patch Antenna Loaded with Split Ring Resonator Based Relative Permeability Near Zero as Superstrate*, Vol. 96, 22389–22399, Springer, Sept. 2017.
25. Aggarwal, I., S. Pandey, and M. R. Tripathy, "A high gain super wideband metamaterial based antenna," *J. Microw. Optoelectron. Electromagn. Application*, Vol. 20, No. 2, 248–273, Jun. 2021.
26. Sumathi, K., S. Lavadiya, P. Yin, J. Parmar, and S. K. Patel, "High gain multiband and frequency reconfigurable metamaterial superstrate microstrip patch antenna for C/X/Ku band wireless network applications," *Wireless Networks*, Vol. 27, 2131–2146, 2021.